

Plastic Optical Fiber Sensor Based on In-fiber Rectangular Hole for Mercury Detection in Water

Jaehee Park* and Hyejin Seo

Department of Electronic Engineering, Keimyung University,
1095, Dalgubeol-daero, Dalseo-gu, Daegu 42601, Korea

(Received January 21, 2020; accepted May 19, 2020)

Keywords: optical fiber sensor, mercury detection, in-fiber hole, rhodamine, chemical sensor

In this study, the characteristics of a plastic optical fiber (POF) sensor based on an in-fiber rectangular hole for detecting mercury in water were investigated. The proposed sensor comprises a POF that includes an in-fiber rectangular hole partially filled with a synthesized rhodamine derivative acting as a sensing probe. The rhodamine derivative with maximum absorbance spectrum variations occurring at approximately 530 nm was fabricated from rhodamine 6G of 95% purity, and the in-fiber rectangular hole with dimensions of $3 \times 0.65 \text{ mm}^2$ was fabricated using an inexpensive drilling machine. The thickness of the rhodamine derivative attached to the rectangular hole was about 0.5 mm. The absorbance of the mercury-detecting POF sensor was proportional to the mercury ion concentration. The relationship between the absorbance and the mercury ion concentration was approximately linear in the mercury ion concentration range of 10 to 200 ppm. The sensitivity was about 0.00031 ppm^{-1} in the linear response region. The experimental results show that the proposed POF sensor can be effectively used to detect mercury ions in water.

1. Introduction

Mercury is a known environmental pollutant routinely released from coal-burning power plants, oceanic and volcanic emissions, gold mining, and solid waste incineration. The long atmospheric residence time of mercury vapor and its oxidation to soluble inorganic mercury provide a pathway for contaminating vast amounts of water and soil. Exposure to mercury can be harmful to the brain, heart, kidneys, lungs, and immune system of people of all ages. Thus, the development of detection techniques for the real-time and long-term monitoring of mercury contamination in environmental and biological samples remains a high priority.^(1,2)

Standard methods for detecting the presence of mercury in water include cold-vapor atomic fluorescence detection and inductively coupled plasma techniques.⁽³⁾ However, these methods require bulky and expensive detection equipment, a large sample volume, and a long process. Hence, using optical fiber sensors for mercury detection has attracted significant attention because of advantages, such as short measurement time, electromagnetic interference immunity,

*Corresponding author: e-mail: jpark@kmu.ac.kr
<https://doi.org/10.18494/SAM.2020.2773>

simplicity, and low cost.^(4–7) Most optical fiber sensors for mercury detection have been based on silica fibers, which are highly sensitive; however, their performance is severely affected by ambient noise conditions such as temperature variation, pressure variation, and vibration. Thus, plastic optical fiber (POF) sensors have also been developed for mercury detection in aqueous environments^(8,9) because they are unaffected by ambient noise although they are less sensitive.⁽¹⁰⁾ Mercury-detecting POF sensors have additional merits over mercury-detecting glass fiber sensors, such as high elastic strain limit, easy handling, high fracture toughness, high flexibility in bending, high sensitivity to strain, and potentially negative thermo-optic coefficients.^(11–13) Unfortunately, most developed mercury-detecting POF sensors are not suitable for use in the field because they are fragile and require complex equipment. There is still a strong industrial need for a low-cost and portable alternative for mercury detection using POF sensors.

POF sensors based on in-fiber microholes have recently attracted interest because of their simple structure, low cost, high tensile strength, and easy handling. These sensors have already been used for refractive index,⁽¹⁴⁾ liquid level,⁽¹⁵⁾ and respiration rate⁽¹⁶⁾ measurements, and previous research studies have shown that they may be suitable for mercury detection. Accordingly, in this study, the characteristics of a POF sensor (Fig. 1) based on an in-fiber rectangular hole partially filled with a rhodamine derivative acting as a sensing probe for detecting mercury were investigated. When this POF sensor is placed in water contaminated with mercury, the contaminated water flows through the rectangular hole and the interaction between the mercury ion in water and the rhodamine derivative attached to the rectangular hole occurs. The light propagating in the rectangular hole is absorbed through the ring opening of the rhodamine derivative induced by mercury ions in water.

2. Theory

Figure 2 shows the schematic diagram of a POF with an in-fiber rectangular hole. For a step index POF with a large diameter core, more than one million modes at 530 nm are used in the experiment. Therefore, an analysis should be conducted from the ray optics perspective.⁽¹⁵⁾ Because the fiber is cylindrically symmetrical, we only need to consider the upper half of the fiber axis.

The transmittance equation of the POF with an in-fiber rectangular hole is derived with the assumption that the material in the rectangular hole is water for simplicity. The refractive index of water (1.3338) is less than those of the cladding (1.41) and core (1.49). The light between θ_2 [$= \tan^{-1}(h/2L)$], the angle of ray B subtended at L [$= r \tan(\theta_c)$] by the hole, and θ_3 [$= \tan^{-1}(r/L)$],

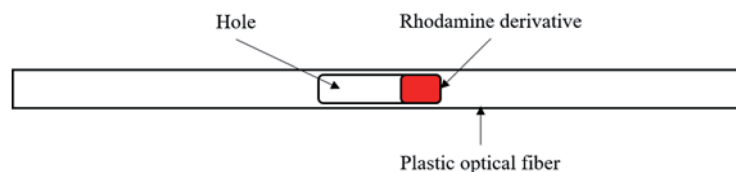


Fig. 1. (Color online) Schematic diagram of a POF sensor for mercury detection.

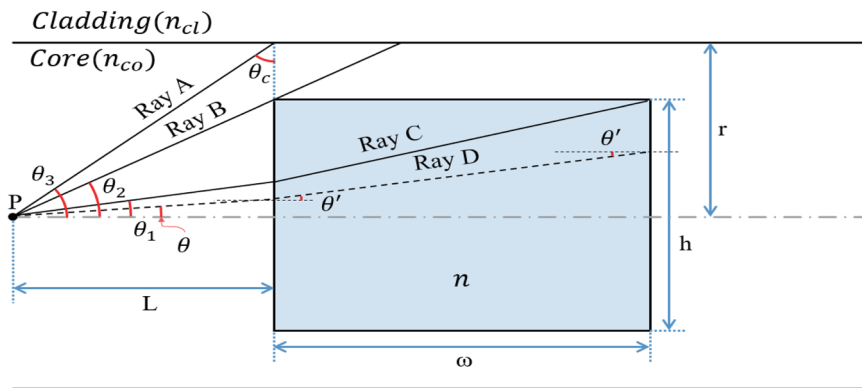


Fig. 2. (Color online) Schematic diagram of a POF with an in-fiber rectangular hole.

the complementary critical angle corresponding to ray A, can be assumed to propagate without loss because it is not blocked by the hole and it causes total internal reflections at the interface between the core and the cladding and at the interface between the core and the material inside the hole. The height of the hole is h , the radius of the core is r , the critical angle between the core and the cladding is $\theta_c [= \sin^{-1}(n_{co}/n_{cl})]$, the refractive index of the core is n_{co} , and the refractive index of the cladding is n_{cl} . The light between θ_2 and θ_1 , the angle of ray C, which reaches the corner or top interface between the core and the material in the rectangular hole after refracting at the left interface, cannot travel in the core because the incident angle of the ray at the core–cladding interface is less than the critical angle. The angle θ_1 can be calculated as

$$w \tan \left[\sin^{-1} \left(\frac{n_{co}}{n} \sin \theta_1 \right) \right] + L \tan \theta_1 = h / 2. \quad (1)$$

The light below θ_1 , ray D, can pass through the left and right interfaces and propagate. The transmittance can be simply obtained by assuming the following:

- (1) Because the index difference between the fiber core and the material inside the rectangular hole is very small, Fresnel reflections at the input and output materials into the rectangular hole/fiber core boundaries are ignored,
- (2) only meridional rays are considered,
- (3) the mode distribution is uniform, and
- (4) there is no scattering from the hole surface roughness.

Therefore, the transmittance becomes

$$T = \frac{(\theta_3 - \theta_2) + \theta_1}{\theta_3}. \quad (2)$$

Equation (2) indicates that the transmittance of the POF with the rectangular hole depends on the rectangular hole size, the core radius, and the refractive indices of the material, cladding, and core.

A mercury-detecting POF sensor is composed of a POF including an in-fiber rectangular hole partially filled with a rhodamine derivative (refractive index = $1.19 + j0.322$). To analyze the performance of this mercury-detecting POF sensor, two consecutive rectangular holes filled with water and the rhodamine derivative should be considered. The transmittance at any mercury concentration in water is

$$T_s = T_1 T_2 - \alpha, \quad (3)$$

where T_1 is the transmittance of the first rectangular hole filled with water between the core and the rhodamine derivative, T_2 is the transmittance of the second rectangular hole occupied with the rhodamine derivative between water and the core, and α is the normalized absorbance at the rhodamine derivative attached to the rectangular hole. The absorbance effect induced by mercury in water can be extracted by subtracting the transmittance at a mercury concentration of 0 ppm from the transmittance at any concentration. Because the absorbance is 0 at the mercury concentration of 0 ppm, the absorbance is expressed as

$$\alpha = T_0 - T_s, \quad (4)$$

where T_0 is the transmittance at the mercury concentration of 0 ppm.

3. Sensor Fabrication and Experiments

Rhodamine derivatives as fluorophore and chromophore probes have attracted considerable interest because of their excellent photophysical properties.⁽¹⁷⁾ Rhodamine derivatives are non-fluorescent and colorless, whereas the ring opening of the corresponding spirolactam gives rise to a strong fluorescence emission and a pink color. When rhodamine binds mercury ions in an aqueous solution, the ring opening process is induced. Therefore, in this study, we used a rhodamine derivative as a chromophore probe.

To synthesize the rhodamine derivative (Fig. 3), rhodamine 6G (958 mg, 2 mmol) was dissolved in ethanol (20 ml) and ethylenediamine (0.67 ml, 10 mmol), and the mixture was then refluxed for about 21 h. Next, the mixture solution was cooled and filtered to collect the precipitate, which was washed in ethanol. The precipitate was then mixed with an acetonitrile solvent (30 ml) to remove any impurities, recrystallized, and filtered to obtain the rhodamine derivative.

A gel-type rhodamine derivative was obtained by the sol-gel method, where a powder-type rhodamine derivative was mixed with tetramethyl orthosilicate (24 ml), trimethoxy methylsilane (6 ml), H₂O (7.5 ml), and ethanol (30 ml), and stirred for 2 h. Table 1 shows the conditions used to synthesize the rhodamine derivative. Using the above procedure, three different rhodamine derivatives were fabricated from rhodamine 6G of 90, 95, and 99% purities to choose the optimal material for detecting mercury ions in water.

The absorption spectra of three different rhodamine derivatives were measured according to the mercury concentration using a spectrometer (Shimadzu UV-1800). The absorption was read while changing the wavelength of the spectrometer after adding the powder-type rhodamine

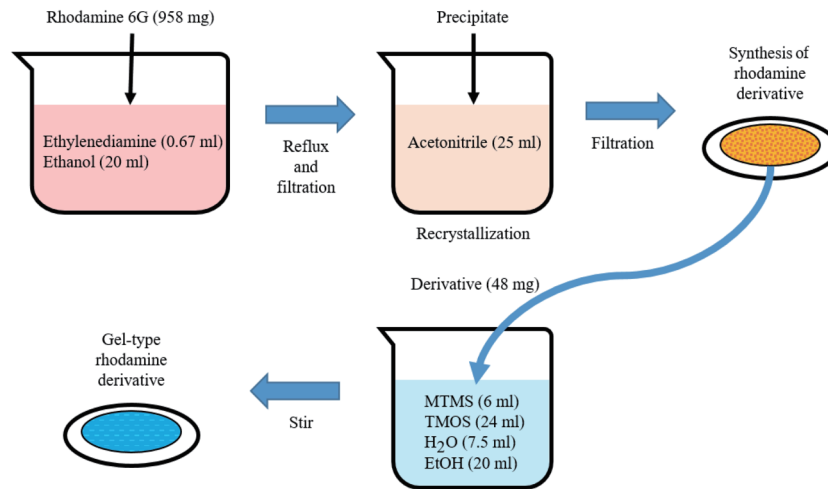


Fig. 3. (Color online) Flow diagram of the rhodamine derivative synthesis.

Table 1
Synthesis conditions for rhodamine derivatives.⁽¹⁴⁾

Item	Value
Reflux temperature (°C)	70
Reflux time (h)	21
Additional solvent amount (ml)	25
Recrystallization time (min)	30
Yield (%)	96.7

derivative to the mercury solution at any concentration in a transparent cell. Figures 4(a)–4(c) show the absorption graphs for the rhodamine derivatives synthesized from rhodamine 6G of 90% purity (Avention), 95% purity (Avention), and 99% purity (Sigma Aldrich). As shown, the absorbance varied in the wavelength range from 500 to 560 nm according to the mercury concentration, with the largest absorbance variation observed at around 530 nm. Figure 4 also shows that the absorption variation was proportional to the purity of rhodamine 6G. The experimental results demonstrate that rhodamine derivatives can be used as sensing probes for detecting mercury ions in water. Despite the largest absorbance variation of the rhodamine derivative synthesized from rhodamine 6G of 99% purity, the rhodamine derivative synthesized from rhodamine 6G of 95% purity was chosen as the sensing probe, in consideration of sensitivity and cost. In this research, the rhodamine derivative of 0.5 mm thickness was inserted into the in-fiber rectangular hole for detecting mercury.

To fabricate the mercury-detecting POF sensor, a $3 \times 0.65 \text{ mm}^2$ in-fiber rectangular air hole was fabricated in the POF using an inexpensive drilling machine (SMC HD-280), a microdrill bit (NEO Technical System), a 532 nm laser diode (LD), and a power meter (PM) (Fig. 5).⁽¹⁵⁾ The gel-type rhodamine derivative of about 0.5 mm thickness was then inserted into the in-fiber rectangular hole and bonded to it with epoxy. Finally, the part filled with the rhodamine derivative was wound using Teflon tape. The POF used in this experiment had a core diameter

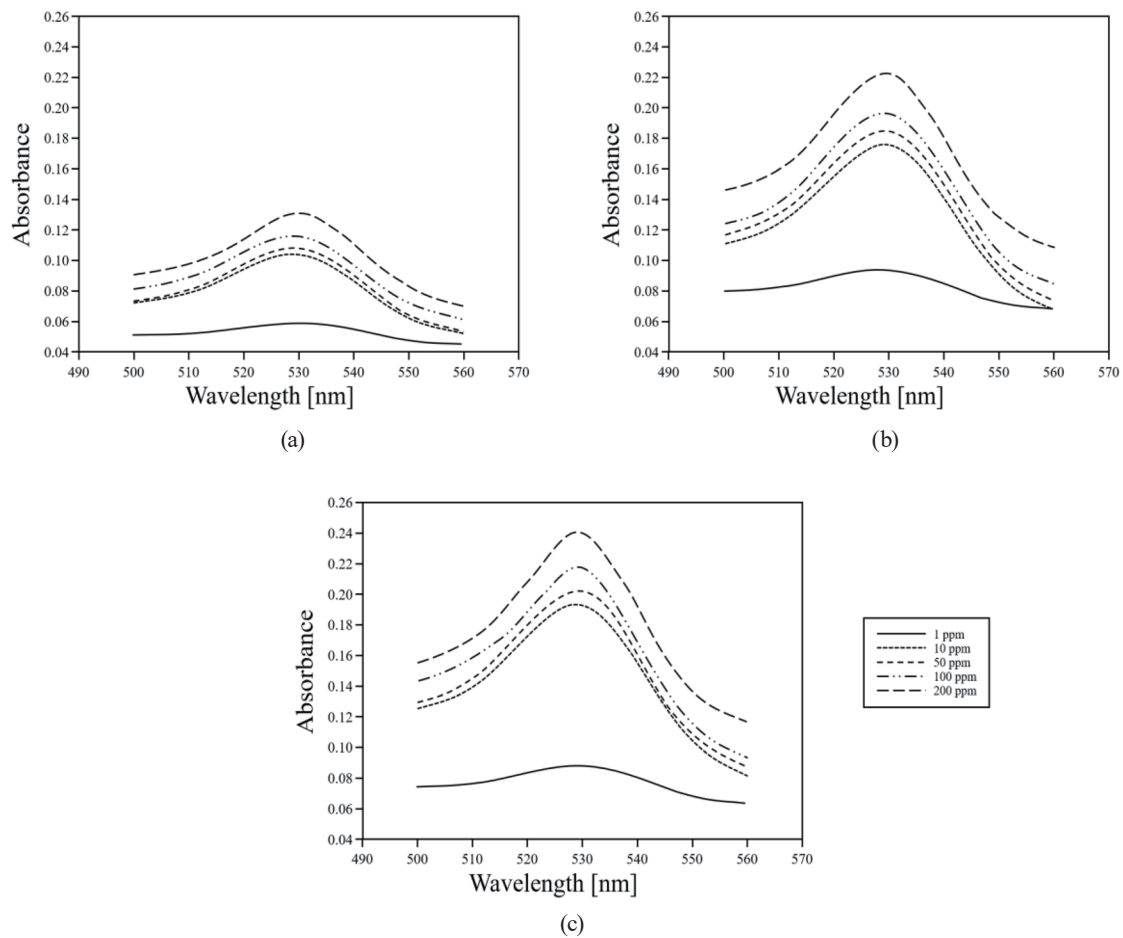


Fig. 4. Absorbance of rhodamine derivatives synthesized from rhodamine 6G of (a) 90, (b) 95, and (c) 99% purities.

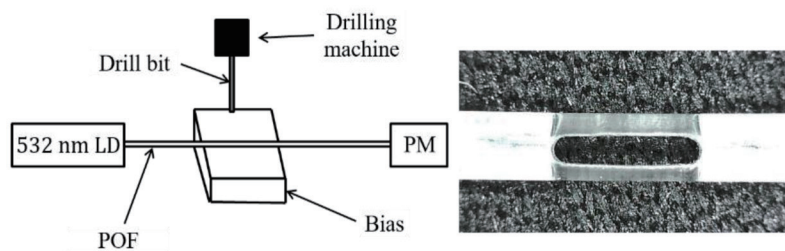


Fig. 5. Fabrication setup and in-fiber rectangular hole in the POF.

of 1.48 mm and core and cladding indices of 1.49 and 1.41, respectively. The insertion loss of the POF mercury-detecting POF sensor was about 3 dB. The photograph on the right-hand side of Fig. 5 shows the in-fiber rectangular hole fabricated using the drilling machine.

The experimental setup (Fig. 6) for analyzing the characteristics of the mercury-detecting POF sensor consisted of a 532 nm continuous wave laser diode (LD, Edmund Optics 37-027), a power meter (PM, Thorlabs PM100D), and a cylinder equipped with the mercury-detecting

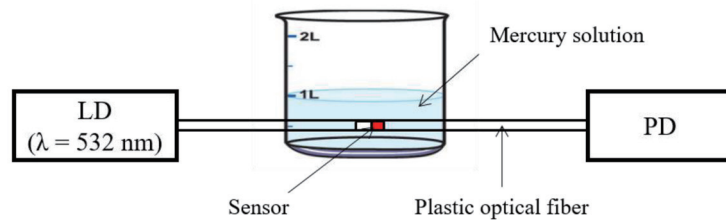


Fig. 6. (Color online) Experimental setup.

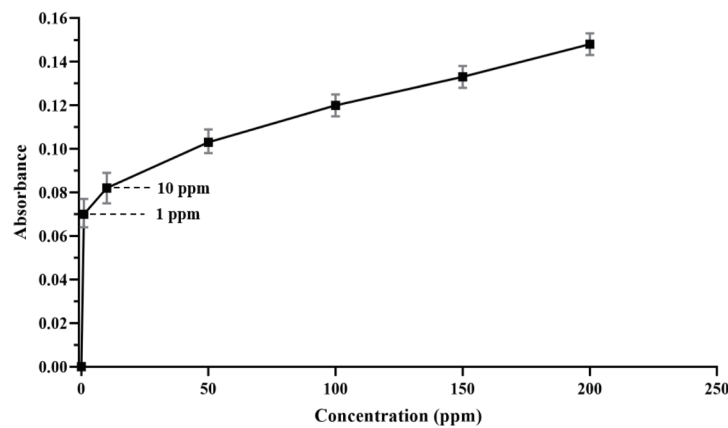


Fig. 7. Absorbance of the mercury-detecting POF sensor.

POF sensor. The light from the laser was coupled into the POF and travelled to the end. At the end of the POF, the optical power was read using the optical power meter about two minutes later after changing the mercury ion concentration induced by putting an adequate quantity of a 1000 ppm mercury standard solution (Kanto Chemical Co.) in distilled water. The quantity of mercury was calculated using the dilution equation $N_1 \cdot V_1 = N_2 \cdot V_2$, where N_1 is the initial concentration of mercury, N_2 is the final concentration, V_1 is the required volume of mercury solution at the initial concentration, and V_2 is the final volume of solution. When the POF sensor was placed in water contaminated with mercury, the coupled light that arrived at the rhodamine derivative inside the in-fiber rectangular hole was absorbed through the ring opening of the rhodamine derivative induced by mercury ions in water. The absorbance changed with the mercury ion concentration in water. The mercury ion concentration was obtained with the absorbance calculated from the optical power measured at the end of the POF. Five mercury-detecting POF sensors were used to measure the mercury ion concentration in water.

Figure 7 shows the graph of the absolute normalized absorbance calculated using $(P_0 - P_m)/P_0$, where P_0 is the measured power when the mercury concentration is 0 ppm and P_m is the measured power at any mercury concentration. The dot is the average measurement value, and the top and bottom are the maximum and the minimum values, respectively. The absorbance of the mercury-detecting POF sensor was proportional to the mercury concentration in an aqueous solution. The absorbance of the mercury-detecting POF sensor increased abruptly at the mercury ion concentration of 1 ppm. After 10 ppm, the absorbance changed

linearly according to the mercury ion concentration in water. The sensor sensitivity was about 0.00031 ppm^{-1} in the linear response region. The experimental results demonstrated that the proposed POF sensor can be effectively used to detect mercury in water.

4. Conclusions

In this study, a POF sensor for detecting mercury in water was demonstrated. This mercury-detecting POF sensor consists of a POF including an in-fiber rectangular hole partially filled with a rhodamine derivative acting as a sensing probe. The rhodamine derivative was fabricated from 95%-pure rhodamine 6G, in consideration of sensitivity and cost, and the rectangular hole of the POF was produced using an inexpensive drilling machine. The dimensions of the fabricated rectangular hole of the POF were $3 \times 0.65 \text{ mm}^2$ and the thickness of the rhodamine derivative attached to the rectangular hole was about 0.5 mm. The absorption of the mercury-detecting POF sensor increased with the mercury ion concentration in water. The absorbance of the mercury-detecting POF sensor changed abruptly at the mercury ion concentration of 1 ppm. After 10 ppm, the absorbance increased linearly with the mercury ion concentration in water. The sensing sensitivity was about 0.0031 (1/ppm) from 10 to 200 ppm in the mercury concentration range. The experimental results demonstrate that the proposed POF sensor can be used to detect mercury ions in water. For a more accurate measurement, the dependence of the POF sensor performance on the pH and temperature of the solution should be studied. Furthermore, research should also focus on increasing the sensitivity of the proposed POF sensor to measure mercury ion concentration below 1 ppm.

Acknowledgments

This work was supported by a National Research Foundation of Korea (NRF) grant funded by the Korea government (MIST), No. 2018R1D1A1B07048066.

References

- 1 G. Darbha, A. Ray, and P. Ray: *ACS Nano* **1** (2007) 208. <https://doi.org/10.1021/nn7001954>
- 2 Q. Wei, R. Nagi, K. Sadeghi, S. Feng, E. Yan, S. Ki, R. Caire, D. Tseng, and A. Ozcan: *ACS Nano* **8** (2014) 1121. <https://doi.org/10.1021/nn406571t>
- 3 J. Wuilloud, R. Wuilloud, M. Silva, R. Olsina, and L. Martinez: *Spectrochim. Acta, Part B* **57** (2002) 365. [https://doi.org/10.1016/S0584-8547\(01\)00393-7](https://doi.org/10.1016/S0584-8547(01)00393-7)
- 4 N. Hanumegowda, I. White, and X. Fan: *Sens. Actuators, B* **120** (2006) 207. <https://doi.org/10.1016/j.snb.2006.02.011>
- 5 S. Kim, J. Park, and W. Han: *Microwave and Optical Technol. Lett.* **51** (2009) 1689. <https://doi.org/10.1002/mop.24434>
- 6 T. Nguyen, T. Sun, and K. Grattan: *Sensors* **19** (2019) 2142. <https://doi.org/10.3390/s19092142>
- 7 H. Joe, H. Yun, S. Jo, M. Jun and B. Min: *Int. J. Precision Eng. Manufacturing-Green Technol.* **5** (2018) 173. <https://doi.org/10.1007/s40684-018-0017-6>
- 8 D. Raj, S. Prasanth, T. Vineeshkumar, and C. Sudarsanakumar: *Opt. Commun.* **367** (2016) 102. <https://doi.org/10.1016/j.optcom.2016.01.027>
- 9 A. Lee, Y. Kim, B. Kim, and B. Park: *J. Sens. Sci. Technol.* **23** (2014) 173. <https://doi.org/10.5369/JSST.2014.23.3.173>
- 10 J. Crosby, D. Lucas, and C. Koshland: *Sens. Actuators, B* **181** (2013) 938. <https://doi.org/10.1016/j.snb.2013.02.037>

- 11 J. Park: Opt. Eng. **50** (2011) 020501. <https://doi.org/10.1117/1.3542040>
- 12 A. Armin, M. Soltanolkotabi, and P. Feizollah: Sens. Actuators, A **165** (2011) 181. <https://doi.org/10.1016/j.sna.2010.10.006>
- 13 A. Grillet, D. Kinet, J. Witt, M. Schukar, K. Krebber, F. Poritte, and A. Depra: IEEE Sens. J. **8** (2008) 1215. [10.1109/JSEN.2008.926518](https://doi.org/10.1109/JSEN.2008.926518)
- 14 J. Shin and J. Park: IEEE Photonics Technol. Lett. **25** (2013) 1882. [10.1109/LPT.2013.2278973](https://doi.org/10.1109/LPT.2013.2278973)
- 15 J. Park, Y. Park, and J. Shin: Jpn. J. Appl. Phys. **54** (2015) 028002. <https://doi.org/10.7567/JJAP.54.028002>
- 16 D. Ahn, Y. Park, J. Shin, J. Lee, and J. Park: Microwave Opt. Technol. Lett. **61** (2019) 120. <https://doi.org/10.1002/mop.31524>
- 17 H. Kim, M. Lee, H. Kim, J. Kim, and J. Yoon: Chem. Soc. Rev. **37** (2008) 1465. <https://doi.org/10.1039/B802497A>

About the Authors



Jaehye Park received his B.S. degree from Kyungpook National University, Korea, in 1984 and his M.S. and Ph.D. degrees from Texas A&M University, USA, in 1992 and 1995, respectively. From 1984 to 1990, he was a researcher at the Agency for Defense Development, Korea. From 1995 to 1997, he was a general manager for Samsung Electro-Mechanics, Korea. Since 1997, he has been a professor at Keimyung University. His research interests are in optical fiber sensors and optical signal processing. (jpark@kmu.ac.kr)



Hyejin Seo received her B.S. degree from Keimyung University, Korea, in 2020. Since 2020, she has been a master student and a research assistant at Keimyung University. Her research interests are in optical fiber sensors and optical signal processing. (hjseo.ec@gmail.com)